11-8-2019

Understanding the Synthesis of Supported Vanadium Oxide Catalysts using Chemical Grafting

Alyssa M. Love
University of Wisconsin-Madison

Melissa C. Cendejas
University of Wisconsin-Madison

Michael P. Hanrahan
Iowa State University, mph@iastate.edu

Scott L. Carnahan
Iowa State University, scottc@iastate.edu

Pajean Uchupalanun
University of Wisconsin-Madison

See next page for additional authors

Understanding the Synthesis of Supported Vanadium Oxide Catalysts using Chemical Grafting

Abstract

The complexity of variables during incipient wetness impregnation synthesis of supported metal oxides precludes an in-depth understanding of the chemical reactions governing the formation of the dispersed oxide sites. This contribution describes the use of vapor phase deposition chemistry (also known as grafting) as a tool to systematically investigate the influence of isopropanol solvent on VO(OiPr)3 anchoring during synthesis of vanadium oxide on silica. We find that the availability of anchoring sites on silica not only depends on the pretreatment of the silica but also on the solvent present. H-bond donors can reduce the reactivity of isolated silanols whereas disruption of silanol nests by H-bond acceptors can turn unreactive H-bonded silanols into reactive anchoring sites. The model suggested here can inform improved syntheses with increased dispersion of metal oxides on silica.

Keywords

heterogeneous catalysis, selective oxidation catalyst, preparation NMR

Disciplines

Catalysis and Reaction Engineering | Chemistry

Authors

Alyssa M. Love, Melissa C. Cendejas, Michael P. Hanrahan, Scott L. Carnahan, Pajean Uchupalanun, Aaron J. Rossini, and Ive Hermans

CHEMISTRY
A European Journal

A Journal of
ChemPubSoc Europe

Accepted Article

Title: Understanding the Synthesis of Supported Vanadium Oxide Catalysts using Chemical Grafting

Authors: Alyssa M. Love, Melissa C. Cendejas, Michael P. Hanrahan, Scott L. Carnahan, Pajean Uchupalanun, Aaron J. Rossini, and Ive Hermans

To be cited as: *Chem. Eur. J.* 10.1002/chem.201904260

Link to VoR: http://dx.doi.org/10.1002/chem.201904260

Supported by
ACES

WILEY-VCH

10.1002/chem.201904260

WILEY-VCH

FULL PAPER

Understanding the Synthesis of Supported Vanadium Oxide Catalysts using Chemical Grafting

Alyssa M. Love,‡[a] Melissa C. Cendejas,‡[a] Michael P. Hanrahan,[c] Scott L. Carnahan,[c] Pajean Uchupalanun,[a] Aaron J. Rossini,[c]* Ive Hermans[a],[b],*

Abstract: The complexity of variables during incipient wetness impregnation synthesis of supported metal oxides precludes an in-depth understanding of the chemical reactions governing the formation of the dispersed oxide sites. This contribution describes the use of vapor phase deposition chemistry (also known as grafting) as a tool to systematically investigate the influence of isopropanol solvent on $VO(O_iPr)_3$ anchoring during synthesis of vanadium oxide on silica. We find that the availability of anchoring sites on silica not only depends on the pretreatment of the silica but also on the solvent present. H-bond donors can reduce the reactivity of isolated silanols whereas disruption of silanol nests by H-bond acceptors can turn unreactive H-bonded silanols into reactive anchoring sites. The model suggested here can inform improved syntheses with increased dispersion of metal oxides on silica.

Introduction

Controlling the speciation of surface-bound active sites on supported catalysts presents a synthetic challenge in heterogeneous catalysis. For supported metal oxide catalysts, the structure of metal oxide sites on the support surface has a significant impact on the performance of the catalyst.[1] For example, silica-supported vanadium oxide – a catalyst widely studied for the oxidative dehydrogenation of propane (ODHP) to propene – has a higher selectivity towards propene when the catalyst surface is comprised solely of dispersed, two-dimensional VO_x surface species. Conversely, as the loading of vanadium oxide is increased beyond a certain threshold, three-dimensional V_2O_5 particles begin to form which lower the catalyst selectivity towards propene in favor of CO_x overoxidation products.[1] Clearly for this catalytic application, understanding the variables that could maximize the dispersion of two-dimensional metal oxide species on a support surface would be invaluable towards improving the preparation of these catalysts.

Wet impregnation is one of the most common synthetic techniques for the synthesis of supported metal oxide catalysts. For the synthesis of supported metal oxides, a metal alkoxide precursor is typically dissolved in its corresponding alcohol solvent and then added dropwise to a solid support. For example, vanadium oxytriisopropoxide ($VO(O_iPr)_3$) dissolved in isopropanol is a common precursor solution used for the wet impregnation synthesis of supported vanadium oxide catalysts.[1-2] If the amount of solution added to the solid is enough to create a slurry of the precursor solution and support, then the synthesis is considered a wet impregnation. If the volume of the solution added is only enough to wet the surface of the material (*i.e.*, the mixture is still mostly dry), then the synthesis is considered an incipient wetness impregnation. After this step the solution/support mixture is calcined at high temperatures (> 500 °C) to yield the final supported metal oxide.[3] A detailed understanding of the chemical reactions controlling the favorable dispersion of metal oxides on materials prepared by impregnation presents a significant challenge, given the complexity of variables to consider in this system. To address this challenge, this contribution describes the use of vapor phase deposition synthesis techniques to systematically investigate the influence of key synthesis variables – solvent and support surface composition – on the dispersion of surface vanadium sites on the surface of silica.

To date, a number of studies have utilized grafting and vapor phase deposition strategies to synthesize supported vanadium oxide catalysts.[4] Previously, our group has demonstrated for the case of silica supported vanadium oxide that grafting can be used as a tool to understand the dispersion of supported metal oxide sites.[5] By grafting the neat vanadium precursor, $VO(O_iPr)_3$, to silica dehydrated at 700 °C (called $V/SiO_{2(700)}$), we significantly decreased the complexity of variables in our synthesis (compared to incipient wetness), and were able to characterize key chemical reactions governing the formation of vanadium oxide sites on silica. We determined that $VO(O_iPr)_3$ anchors to both silanol and strained siloxane bridges on $SiO_{2(700)}$. We characterized the structure of two distinct vanadium sites after grafting using ^{13}C and ^{51}V solid-state magic angle spinning (MAS) NMR. A recent work by Mance and Coperet details how proton detected fast MAS experiments can be used to characterize supported vanadium oxide catalysts. They reach similar conclusions regarding the structure of the supported vanadium species.[6] Thermogravimetric analysis-differential scanning calorimetry-mass spectrometry (TGA-DSC-MS) of the calcination of $V/SiO_{2(700)}$ revealed that the material undergoes an endothermic restructuring process starting around 200 °C, at which point both propene and water molecules are released from the surface of the material. A combination of *in situ* Raman and Diffuse Reflectance Fourier Transform Infrared spectroscopy (DRIFTS) analyses of the calcination showed that a transient V-

[a] Dr. AM Love, MC Cendejas, P Uchupalanun, and Prof. Dr. I Hermans
Department of Chemistry
University of Wisconsin – Madison
1101 University Avenue, Madison, WI, 53706 USA
E-mail: hermans@chem.wisc.edu
[b] Prof. Dr. I Hermans
Department of Chemical and Biological Engineering
University of Wisconsin – Madison
1415 Engineering Drive, Madison WI 53706, USA
[c] MP Hanrahan, SL Carnahan, and Prof. Dr. AJ Rossini
Department of Chemistry
Iowa State University
1605 Gilman Hall, Ames, IA 50011, USA

‡ AM Love and MC Cendejas contributed equally to this work.

Supporting information for this article is given via a link at the end of the document.

10.1002/chem.201904260

OH species appears at intermediate temperatures (200-400 °C; observed in DRIFTS), while the vanadyl stretch (V=O) was preserved throughout the entire calcination (observed *via* Raman spectroscopy). Characterization of the calcined material with ^{51}V MAS NMR revealed that the material contained exclusively dispersed VO_x species. Catalytic testing of this material for ODHP revealed that the material exhibits strikingly similar selectivity and turnover frequency to an analogous material synthesized via incipient wetness impregnation, which solidified this material as a valuable model system for the fundamental study of supported metal oxides.

In this contribution we build upon our previously established grafting methodology to investigate how the presence of alcohol solvent (*i.e.*, isopropanol) during dispersion of a metal alkoxide precursor affects the dispersion of vanadium oxide on silica. We divide our study into three major sections, investigating (i) isopropanol grafting to silica supports, (ii) two-step isopropanol and $VO(O_iPr)_3$ grafting to silica dehydrated at 700 °C ($SiO_{2(700)}$), and (iii) isopropanol and $VO(O_iPr)_3$ grafting to silica dehydrated at 200 °C ($SiO_{2(200)}$). This way, we systematically develop a model that describes how the interaction between isopropanol and silica controls the structure and distribution of surface grafted species.

Results and Discussion

Grafting isopropanol to silica.

To better understand the role of isopropanol on the dispersion of vanadium oxide sites on silica, we first grafted isopropanol to silica and conducted a series of characterization studies on the resultant surface species. We condensed anhydrous isopropanol onto amorphous silica (Aerosil ® 200, BET surface area 200 $m^2 \cdot g^{-1}$) dehydrated at 700 °C and 200 °C under vacuum (called $SiO_{2(700)}$ and $SiO_{2(200)}$, respectively). We also used $SiO_{2(700)}$ silylated with $(TMS)_2NMe$ (to exchange Si-OH groups for Si-O-TMS groups; denoted TMS-$SiO_{2(700)}$) as a support to assess the reactivity of isopropanol exclusively with strained siloxane bridges that exist on the support surface as a result of the 700 °C dehydration temperature.[7] Isopropanol was left to react with the SiO_2 support at room temperature for 30 min. At this stage the materials are denoted $SiO_{2(700)}$+$_i$PrOH, $SiO_{2(200)}$+$_i$PrOH and TMS-$SiO_{2(700)}$+$_i$PrOH, respectively. Following this reaction, the materials were post-treated by heating to 50 °C under dynamic vacuum for 1 h to remove weakly physisorbed isopropanol from the support. The post-treated materials are called $SiO_{2(700)}$+$_i$PrOH$_{(50)}$, $SiO_{2(200)}$+$_i$PrOH$_{(50)}$, and TMS-$SiO_{2(700)}$+$_i$PrOH$_{(50)}$.

Transmission IR spectra were collected at each stage of the synthesis (following both deposition and post-treatment) and are summarized in Figure 1. The spectrum for $SiO_{2(700)}$ in Figure 1a contains a sharp peak at 3745 cm^{-1} and is attributed to the OH stretching for isolated silanol groups.[7a, 8] The features between 2100 and 1500 cm^{-1} are Si-O-Si overtones to which all of the transmission IR spectra are normalized in order to quantitatively compare features between spectra. The IR spectrum for $SiO_{2(700)}$+$_i$PrOH contains a sharp peak at 3744 cm^{-1} at lower intensity than the plain support, in addition to a broad shoulder between ca. 3700 and 3100 cm^{-1} corresponding to H-bonding O-H vibrations,[7a] and several peaks between 3025 and 2850 cm^{-1} corresponding to C-H vibrations from isopropanol (Figure S1). We attribute the decrease in isolated SiOH peak intensity to hydrogen bonding between the SiOH groups and isopropanol –OH groups. After post-treatment at 50 °C under vacuum, the intensities of the shoulder and C-H stretch region decrease slightly in the IR spectrum for $SiO_{2(700)}$+iPrOH$_{(50)}$,

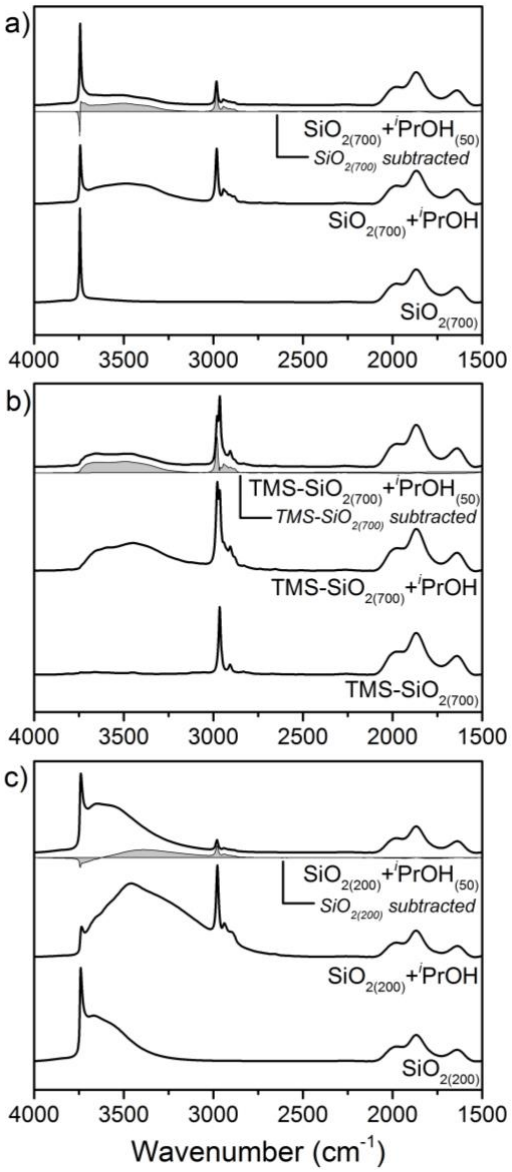

Figure 1. Transmission FTIR spectra for a) $SiO_{2(700)}$ (bottom trace), $SiO_{2(700)}$ condensed with an excess of isopropanol as compared to the silanol content ($SiO_{2(700)}$+$_i$PrOH; middle trace), and $SiO_{2(700)}$+$_i$PrOH after heating under vacuum to 50 °C to remove weakly bound isopropanol species ($SiO_{2(700)}$+$_i$PrOH$_{(50)}$; top trace). The analogous materials prepared on silylated $SiO_{2(700)}$ (TMS-$SiO_{2(700)}$) and SiO_2 dehydrated at 200 °C under vacuum ($SiO_{2(200)}$) are provided in panels b) and c), respectively. Difference spectra between the original support

10.1002/chem.201904260

spectrum and final post treated material are shown as filled gray spectra just below each of the top traces.

which is expected after the removal of weakly physisorbed isopropanol from the support. The difference spectrum (shaded trace) between $SiO_{2(700)}$+$_i$PrOH$_{(50)}$ and $SiO_{2(700)}$ shows that there is a decrease in the intensity of the isolated SiOH peak at 3744 cm^{-1}.

Figure 1b contains a summary of the IR spectra taken at each stage of isopropanol grafting to TMS-$SiO_{2(700)}$. Unlike $SiO_{2(700)}$, the IR spectrum for TMS-$SiO_{2(700)}$ does not exhibit a sharp peak at 3745 cm^{-1} due to the complete reaction of SiOH groups with $(TMS)_2NMe$ to form Si-O-TMS groups. This spectrum also contains several peaks between 3000 and 2870 cm^{-1} that corresponds to the C-H stretches from the surface trimethylsilyl (TMS) groups. Following condensation of isopropanol on the support, the IR spectrum for TMS-$SiO_{2(700)}$+$_i$PrOH shows the appearance of a broad feature between 3750 and 3100 cm^{-1} and an increase in intensity of the features in the C-H stretch region, much like the IR spectrum for $SiO_{2(700)}$+$_i$PrOH. Following post-treatment of TMS-$SiO_{2(700)}$+$_i$PrOH, the IR spectrum of TMS-$SiO_{2(700)}$+$_i$PrOH$_{(50)}$ also shows a decrease in the broad feature centered at ca. 3500 cm^{-1}, as well as a decrease in the C-H stretch region. The difference spectrum between TMS-$SiO_{2(700)}$+$_i$PrOH$_{(50)}$ and the TMS-$SiO_{2(700)}$ support shows that following post-treatment there are still C-H stretches present that come from the isopropanol grafting. We expect that the remaining H-bonded OH signal and C-H stretches result from isopropanol opening strained siloxane bridges on the support surface to create a silanol group hydrogen bonding to an adjacent ≡Si-O-$_i$Pr group according to Scheme 1. Since $SiO_{2(700)}$ also contains siloxane bridges, we expect that much of the hydrogen bonded –OH groups left on $SiO_{2(700)}$+$_i$PrOH$_{(50)}$ (Figure 1a) are also a result of this ring opening process. This observation is in line with previous literature studies on the interaction of alcohols with silica pretreated at temperatures above 350 °C.[9]

Figure 1c shows the IR data for the analogous isopropanol grafting study to $SiO_{2(200)}$. The IR spectrum for $SiO_{2(200)}$ contains an isolated silanol peak at 3741 cm^{-1} as well as an intense shoulder centered at ca. 3600 cm^{-1} that corresponds to hydrogen bonded SiOH groups.[7a] Upon condensation of isopropanol to $SiO_{2(200)}$, the IR spectrum for $SiO_{2(200)}$+$_i$PrOH shows a decrease in isolated SiOH peak intensity as well as the appearance of a very intense, broad feature centered at ca. 3460 cm^{-1}. Again, we also observed the appearance of several peaks between 3020 and 2850 cm^{-1} that correspond to the C-H vibrations from isopropanol. The appearance of the broad feature at 3460 cm^{-1} is likely due to hydrogen bonding between silanols and isopropanol OH groups. After post treatment at 50 °C, the IR spectrum for $SiO_{2(200)}$+$_i$PrOH$_{(50)}$ looks similar to the spectrum for the original $SiO_{2(200)}$ support. The difference spectrum between $SiO_{2(200)}$+$_i$PrOH$_{(50)}$ and $SiO_{2(200)}$ shows there is a slight decrease in isolated SiOH content relative to the original support, in addition to a slight increase in peak intensity around 3400 cm^{-1} in the H-bonded OH region, and some small residual peaks in the C-H stretch region. We believe that based on these observations there is some residual isopropanol still present on $SiO_{2(200)}$+$_i$PrOH$_{(50)}$ that is strongly H-bonded to the silica surface and therefore not removed by the post-treatment step. Since $SiO_{2(200)}$ does not contain highly strained siloxane bridges like $SiO_{2(700)}$, it is unlikely that the residual isopropanol species on the surface of the material are ≡Si-O-$_i$Pr moieties that result from opening siloxane bridges.

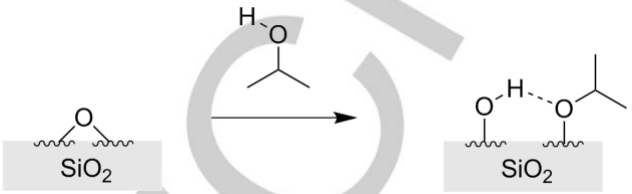

Scheme 1. Illustration of the reaction of isopropanol with a strained siloxane bridge

We also studied the isopropanol-grafted silica materials with TGA-DSC-MS to better characterize the nature of the interaction between the isopropanol and the support. To this end, we heated the samples in aluminum crucibles to 550 °C in air in a TGA-DSC instrument whose outlet was connected to a mass spectrometer. With this experiment we can observe the temperature at which isopropanol species desorbed from the SiO_2 supports to characterize the strength of their interaction with the support (where higher temperatures indicate stronger interactions). The identity of mass fragments detected in the mass spectrometer also provide information about the nature of the desorption process of isopropanol species from the SiO_2 support. Our chosen calcination program is the same as what we have previously used to calcine supported vanadium oxide materials.[1, 5]

Figures 2a-2c show the TGA, DSC, and MS data, respectively, for the calcination of $SiO_{2(700)}$, $SiO_{2(700)}$+$_i$PrOH, and $SiO_{2(700)}$+$_i$PrOH$_{(50)}$. The red TGA trace for $SiO_{2(700)}$+$_i$PrOH (isopropanol condensed onto silica; no post-treatment step) in Figure 2a shows two mass loss steps with onsets at ca. 50 °C and ca. 400 °C. In contrast, the black TGA trace for the post-treated $SiO_{2(700)}$+$_i$PrOH$_{(50)}$ only shows one minor mass loss feature starting at 400 °C. As expected, the TGA trace for $SiO_{2(700)}$ does not show any significant mass loss features upon calcination to 550 °C.

The DSC trace for $SiO_{2(700)}$+$_i$PrOH in Figure 2b shows two features with onsets at 50 °C and 400 °C matching those for the mass loss features in the TGA. Given the conventions for our DSC instrument, the negative peak at 50 °C corresponds to an endothermic transition, whereas the positive peak at 400 °C corresponds to an exothermic transition on the material. The DSC trace for $SiO_{2(700)}$+$_i$PrOH$_{(50)}$ shows a single exothermic transition with an onset just after 400 °C. We expect the features in the TGA-DSC correspond to processes involving the desorption of isopropanol-grafted species; therefore, unsurprisingly we do not observe any exo- or endothermic features in the DSC trace for $SiO_{2(700)}$.

Figure 2c shows the intensities of the major mass fragments (with mass to charge, or m/z, ratios of 18, 44, 42, and 45) observed as a function of temperature during the calcination

10.1002/chem.201904260

process. The identities of these fragments were assigned as H_2O^+, CO_2^+, $C_3H_6^+$, and CH_3CHOH^+ (the most intense mass fragment observed in the mass spectrum for isopropanol), respectively, and are shown to the right of Figure 2c. For the m/z = 42 and 45 fragments, we verified our assignments by looking at the distribution of other minor mass fragments that followed the same intensity profiles as these ions and compared them to the mass spectra of known compounds.[10] We were able to narrow our mass fragment assignments to three-carbon molecules given that we started with isopropanol as our grafting precursor.

When we look at the mass fragments observed as a function of calcination temperature for $SiO_{2(700)}$+*i*PrOH, we observe water, carbon dioxide, propene, and isopropanol desorbing from the surface in the same temperature range as the endothermic process observed at 50 °C. By comparison, we do not observe any mass fragments associated with the plain $SiO_{2(700)}$ support. We assume that this endothermic process arises from the evaporation of isopropanol from the support, since this material has not been post-treated prior to calcination. It also appears that at the same time, some of the isopropanol is decomposing to propene or combusting to form CO_2 and H_2O. The overall feature in the DSC is endothermic, however, because most of the isopropanol must be evaporating so the net heat flow is negative over this temperature range.

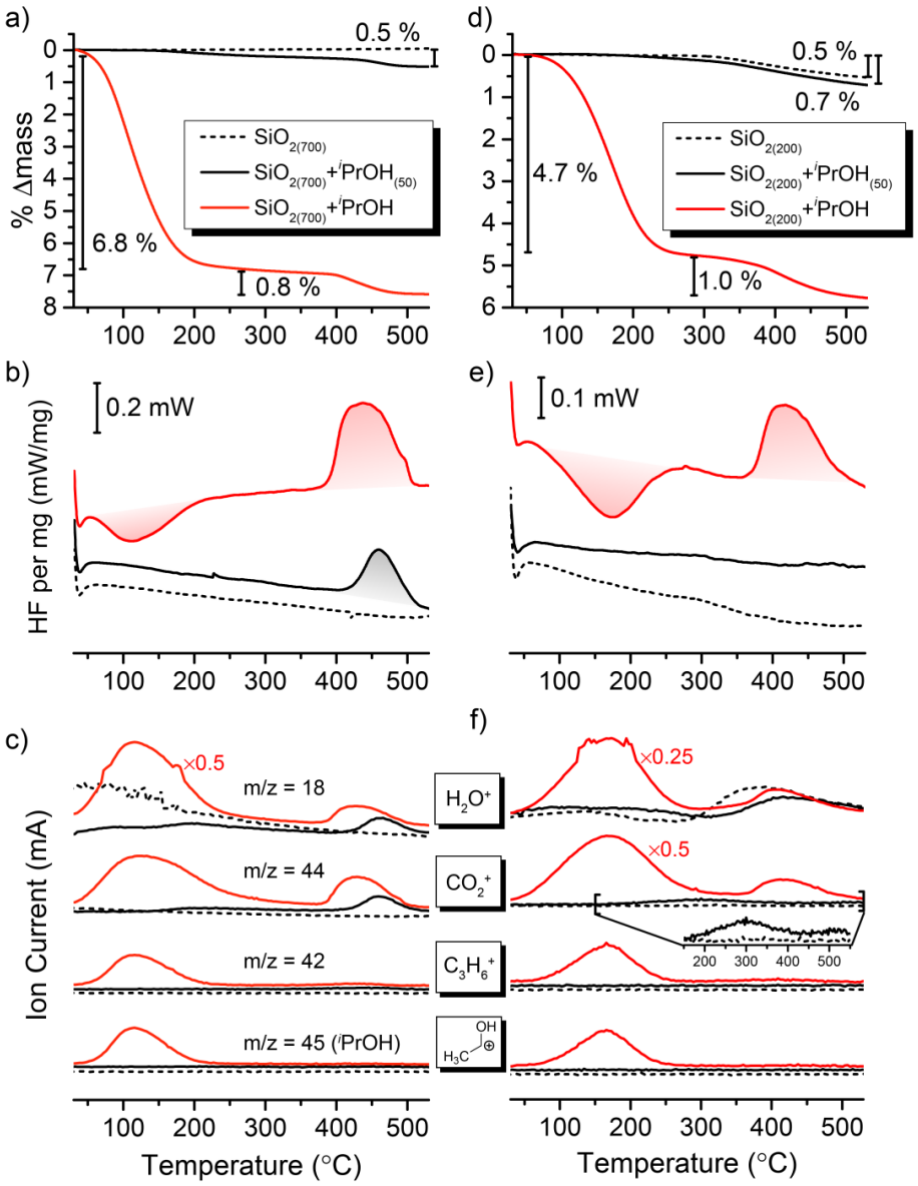

Figure 2. a-c) TGA-DSC-MS traces (respectively) for the calcination of $SiO_{2(700)}$ (dotted line), $SiO_{2(700)}$+*i*PrOH$_{(50)}$ (black line), and $SiO_{2(700)}$+*i*PrOH (red line), to 550 °C in air, d-f) TGA-DSC-MS traces (respectively) for the calcination of $SiO_{2(200)}$ (dotted line), $SiO_{2(200)}$+*i*PrOH$_{(50)}$ (black line), and $SiO_{2(200)}$+*i*PrOH (red line), to 550 °C in air.

10.1002/chem.201904260

For the exothermic process above 400 °C on $SiO_{2(700)}$+$_i$PrOH and the post-treated $SiO_{2(700)}$+$_i$PrOH$_{(50)}$, we observe mass fragments only from CO_2 and H_2O. Based on the onset temperature of this feature and the identity of the mass fragments, we expect that the exothermic feature in both materials arises from the combustion of surface ≡Si-O-$_i$Pr groups. This is consistent with the fact that we know isopropanol can react with strained siloxane bridges on $SiO_{2(700)}$ based on our isopropanol grafting studies with TMS-$SiO_{2(700)}$ (Figure 1b). In addition, we performed TGA-DSC-MS experiments on the same materials heated to 550 °C under N_2 and observed the release of propene from the surface above 400 °C (Figure S2), consistent with the anaerobic decomposition of ≡Si-O-$_i$Pr from the SiO_2 support.

Figures 2d-2f show analogous TGA-DSC-MS data for the calcination of $SiO_{2(200)}$, $SiO_{2(200)}$+$_i$PrOH, and $SiO_{2(200)}$+$_i$PrOH$_{(50)}$ materials. The TGA-DSC-MS data for the non-post treated $SiO_{2(200)}$+$_i$PrOH (red trace) shows very similar characteristics to that of $SiO_{2(700)}$+$_i$PrOH. Based on our previous discussion, we attribute the subsequent endothermic and exothermic processes on this material to the evaporation of isopropanol and the combustion of surface isopropoxide species from the support, respectively. We note here that although we do not expect to observe the formation of ≡Si-O-$_i$Pr species on the surface of $SiO_{2(200)}$ during room temperature grafting, we may observe them during the calcination due to in-situ reaction of physisorbed isopropanol with the silica support.

The TGA trace for post-treated $SiO_{2(200)}$+$_i$PrOH$_{(50)}$ in Figure 2d shows an onset of mass loss starting at ca. 300 °C. The TGA data for the $SiO_{2(200)}$ support has a similar mass loss trace to $SiO_{2(200)}$+$_i$PrOH$_{(50)}$, although $SiO_{2(200)}$+$_i$PrOH$_{(50)}$ has a slightly higher percentage of mass loss compared to the blank support. The DSC traces for both $SiO_{2(200)}$+$_i$PrOH$_{(50)}$ and $SiO_{2(200)}$ in Figure 2d are both relatively flat and contain no major exothermic or endothermic features. When we couple this information with the MS data in Figure 2f, we see that the only major mass fragment observed in these materials comes from water, and matches with the onset temperature of the mass losses in these materials starting around 300 °C. This is consistent with the fact that the supports here were only dehydrated at 200 °C, so further water is driven from the supports at temperatures greater than the original dehydration temperature. In the MS data for $SiO_{2(200)}$+$_i$PrOH$_{(50)}$, we observe a very small amount of CO_2 coming off of the material between 200 °C and 400 °C (Figure 4f, inset). Since this is below the temperature range where we observed the decomposition of ≡Si-O-$_i$Pr groups on the $SiO_{2(700)}$ materials and on $SiO_{2(200)}$+$_i$PrOH, we expect this feature could arise from the combustion of strongly hydrogen-bonded isopropanol species that remain on the material following post-treatment. There are only trace amounts of these species on $SiO_{2(200)}$+$_i$PrOH$_{(50)}$, however, as evidenced by the small percentage of mass (approximately 0.2 %) that these species make up on the material, as well as the very low intensity observed in the C-H stretch region of the IR spectrum for the material (Figure 1c).

To summarize, we conclude that isopropanol reacts with siloxane bridges on $SiO_{2(700)}$ and TMS-$SiO_{2(700)}$ to form silanol groups hydrogen bonded to surface ≡Si-O-$_i$Pr species. The IR spectrum of $SiO_{2(700)}$+$_i$PrOH$_{(50)}$ also suggests some isopropanol hydrogen bonds strongly to isolated silanols such that it is not removed during the post-treatment step. In contrast, isopropanol does not appear to create ≡Si-O-$_i$Pr groups on $SiO_{2(200)}$+iPrOH$_{(50)}$, as no strained siloxane bridges are present on the surface of the $SiO_{2(200)}$ support. We do, however, observe a small trace of what we believe is strongly hydrogen-bonded isopropanol to the surface of $SiO_{2(200)}$+$_i$PrOH$_{(50)}$ following post treatment at 50 °C. We will use these data to inform our interpretation of vanadium and isopropanol grafting experiments detailed in the following sections.

Grafting iPrOH and VO(OiPr)3 to silica.

To understand the effect of alcohol solvent on the dispersion of vanadium oxide, we grafted isopropanol and vanadium oxytriisopropoxide (VO(OiPr)3) in subsequent steps to SiO2(700), TMS-SiO2(700), and SiO2(200). A summary of the two-step grafting procedure is given in Scheme 2. Isopropanol, followed by VO(OiPr)3, are condensed onto the silica support. The isopropanol and VO(OiPr)3 mixture reacts with the support at room temperature and is then heated at 50 °C under dynamic vacuum to remove unreacted precursor and solvent from the support. Materials grafted with both isopropanol and VO(OiPr)3 precursor to SiO2(700), TMS-SiO2(700), and SiO2(200) are denoted V+iPrOH/SiO2(700), V+iPrOH/TMS-SiO2(700), and V+iPrOH/SiO2(200), respectively. Following grafting we characterized these materials with IR spectroscopy in order to verify the complete reaction of isolated silanol groups with precursor molecules (Figure S3).

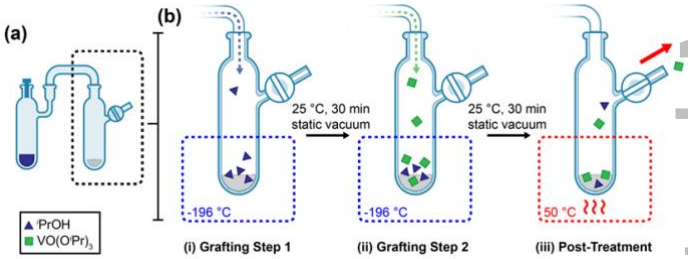

Scheme 2. Experimental setup for the two-step grafting of isopropanol ($_i$PrOH) and VO(O$_i$Pr)$_3$ to silica.

Because this grafting technique is a site-limited reaction – that is, the amount of vanadium that can anchor to the surface is limited by the number of available anchoring sites – we can use the quantification of vanadium content on these materials to assess differences in vanadium precursor anchoring with and without alcohol molecules present. The vanadium loading for V+$_i$PrOH/$SiO_{2(700)}$, V+$_i$PrOH/TMS-$SiO_{2(700)}$, and V+$_i$PrOH/$SiO_{2(200)}$ was determined with ICP-OES and compared to analogous materials grafted with neat VO(O$_i$Pr)$_3$ previously reported by our group (Table 1).[5]

When both VO(O$_i$Pr)$_3$ and isopropanol are grafted to $SiO_{2(700)}$ the vanadium loading is only 2.1 wt.%, while the material with only grafted VO(O$_i$Pr)$_3$ gives 2.9 wt.% vanadium. However, when VO(O$_i$Pr)$_3$ was grafted to TMS-$SiO_{2(700)}$ the vanadium

10.1002/chem.201904260

content was 0.9 wt.% both when neat $VO(O_iPr)_3$ was grafted and when the grafting was performed with isopropanol. This leads us to the important conclusion that the hydrogen bonded silanols formed from the reaction of isopropanol with siloxane bridges are still reactive anchoring sites for the $VO(O_iPr)_3$ precursor. In fact, we observe the consumption of hydrogen-bonded SiOH groups in the IR spectrum for $V+_iPrOH/TMS\text{-}SiO_{2(700)}$ in Figure S3. From this information we also conclude that the decrease in vanadium loading on $V+_iPrOH/SiO_{2(700)}$ must come from blocking of some silanol groups with strongly hydrogen bonding isopropanol, since we know the opened siloxane bridges are still viable anchoring sites. In contrast to the $SiO_{2(700)}$ grafted materials, we observe that the vanadium content on $V+_iPrOH/SiO_{2(200)}$ is 2.7 wt. %, whereas the loading of neat $VO(O_iPr)_3$ grafted to $SiO_{2(200)}$ is lower at 1.6 wt. % V. Although we will predominantly discuss structural characterization of the surface sites on $V+_iPrOH/SiO_{2(700)}$ and $V+_iPrOH/TMS\text{-}SiO_{2(700)}$ materials for the remainder of this section, we will discuss these apparent differences in anchoring behavior for materials grafted on $SiO_{2(200)}$ compared to $SiO_{2(700)}$ at length in the following section.

Table 1. Summary of vanadium elemental analysis (determined by ICP-OES) for materials grafted to $SiO_{2(700)}$, $TMS\text{-}SiO_{2(700)}$, and $SiO_{2(200)}$ with and without an additional isopropanol grafting step.

Support	V Loading (wt. % V)	
	Grafted $VO(O_iPr)_3$	Grafted $_iPrOH + VO(O_iPr)_3$
$SiO_{2(700)}$	2.9 ± 0.2	2.1 ± 0.1
$TMS\text{-}SiO_{2(700)}$	0.9 ± 0.1	0.9 ± 0.1
$SiO_{2(200)}$	1.6 ± 0.3	2.7 ± 0.1

The structure of the resultant surface sites on $V+_iPrOH/SiO_{2(700)}$ and $V+_iPrOH/TMS\text{-}SiO_{2(700)}$ were characterized with magic angle spinning (MAS) solid-state NMR spectroscopy. Figure 3 shows the 1D spin echo ^{51}V spectra for these materials. We note that for consistency, we use site assignments **1** and **2** as defined in our previous work.[5] Peak **1** is assigned to a freely rotating monopodal vanadium site and peak **2** to a vanadium site with a weak fifth coordination that partially inhibits the molecular dynamics that would narrow the ^{51}V NMR signal (Figure 3 inset). Both materials exhibit an isotropic shift centered at –656 ppm for $V+_iPrOH/SiO_{2(700)}$ and –658 ppm for $V+_iPrOH/TMS\text{-}SiO_{2(700)}$ (assigned as **2** in Figure 3 inset). We note that ^{51}V isotropic chemical shifts are not well defined by the coordination number.[11] For example, both tetrahedral and octahedral V sites both have isotropic chemical shifts that range from ca. –500 to –750 ppm.[11] Simulated ^{51}V MAS NMR spectra for $V+_iPrOH/SiO_{2(700)}$ and $V+_iPrOH/TMS\text{-}SiO_{2(700)}$ are given in Figure S4. The simulated spectrum for $V+_iPrOH/SiO_{2(700)}$ exhibits a linewidth of 2.8 kHz for the isotropic peak and a fit of the sideband manifolds indicates a relatively small ^{51}V quadrupolar coupling constant (C_Q) of ca. 560 kHz. For $V+_iPrOH/TMS\text{-}SiO_{2(700)}$ peak **2** has a similar linewidth at 3.5 kHz and a C_Q of 630 kHz (Table S1). The isotropic shift position, linewidth, and C_Q values for peak **2** in the $V+_iPrOH/SiO_{2(700)}$ and $V+_iPrOH/TMS\text{-}SiO_{2(700)}$ spectra are all consistent with a monopodal ^{51}V site with a weak fifth coordination to a nearby $Si\text{-}O\text{-}_iPr$ group (Figure 3, inset), as we have suggested previously.[5] Other groups using different synthesis procedures have proposed a bipodal vanadium site with two surface bonds, however C_Q values were not reported for these species.[4b, 4i]

In previous work, we observed that grafting neat $VO(O_iPr)_3$ to $SiO_{2(700)}$ without isopropanol leads to a ^{51}V isotropic shift at –630 ppm (peak **1**, attributed to an isolated, monopodal vanadium site) *in addition* to the shift observed at –655 ppm.[5] However, in Figure 3 we observe that when both isopropanol and $VO(O_iPr)_3$ are grafted to the surface of silica, only the isotropic shift at ~ –656 ppm corresponding to the asymmetric ^{51}V site is observed, and the signal from monopodal species at –630 ppm is very weak. The lack of fully symmetric, monopodal vanadium sites is likely due to the presence of additional $\equiv Si\text{-}O\text{-}_iPr$ groups on the surface from isopropanol opening siloxane bridges that interact with and distort the geometry of the vanadium sites present on the silica surface.

The increase in $\equiv Si\text{-}O\text{-}_iPr$ species is confirmed by ^{13}C CPMAS NMR (Figure S5) where the intensity of the peak corresponding to the $\equiv Si\text{-}O\text{-}_iPr$ is increased relative to the signal for $V\text{-}O\text{-}_iPr$ when compared to the $V/SiO_{2(700)}$ reported previously. We expect this is due to more $Si\text{-}O\text{-}_iPr$ groups on $V+_iPrOH/SiO_{2(700)}$ that arise from the reaction of isopropanol with strained siloxane bridges, and to the decreased vanadium content on $V+_iPrOH/SiO_{2(700)}$. We also verified our ^{13}C CPMAS assignments with two-dimensional $^1H\text{-}^{29}Si$ HETCOR and $^{51}V \rightarrow {}^1H$ insensitive nuclei enhanced by polarization transfer (INEPT) NMR experiments summarized in Figure S6.

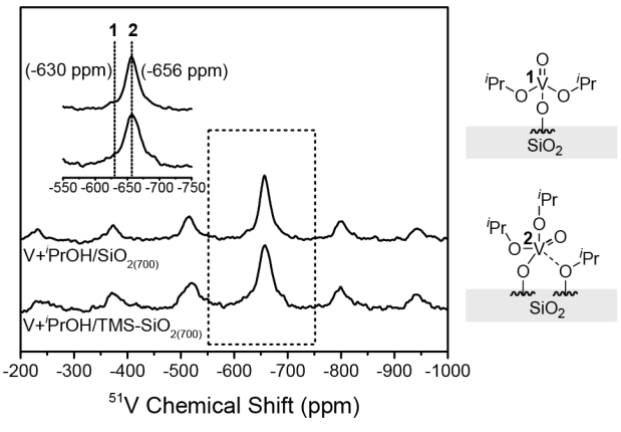

Figure 3. MAS ^{51}V solid-state NMR spectra of $V+_iPrOH/SiO_{2(700)}$ (top) and $V+_iPrOH/TMS\text{-}SiO_{2(700)}$ (bottom). Peak 1 is marked in the ^{51}V MAS NMR spectra, although it is not present, in order to show where the chemical shift for a symmetric, monopodal ^{51}V site would appear.[5]

10.1002/chem.201904260

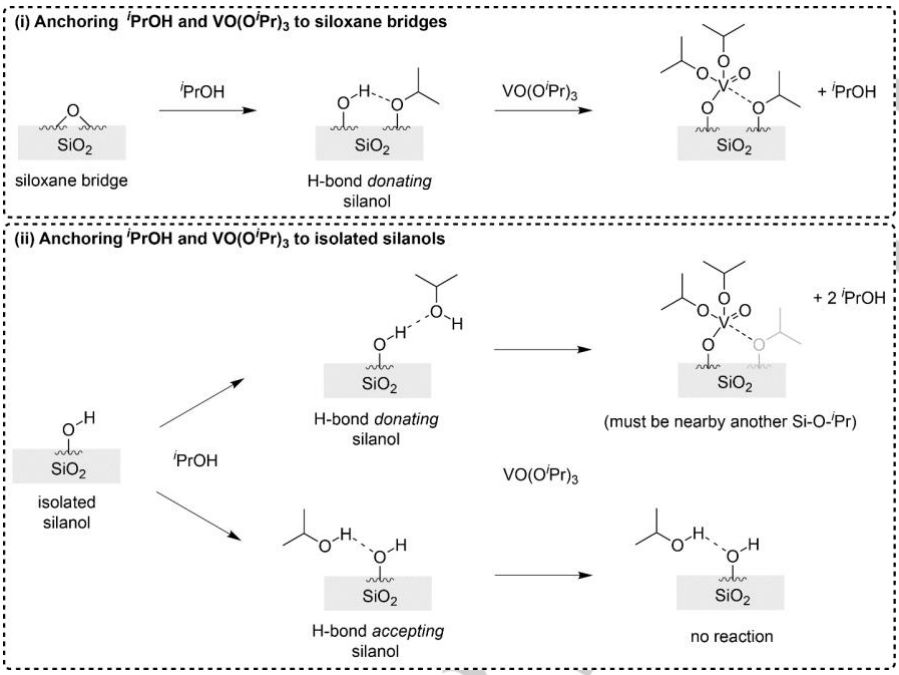

Scheme 3. Proposed reaction pathways for the reaction of $VO(O_iPr)_3$ with SiO_2 in the presence of isopropano

Scheme 3 summarizes the proposed reaction pathways for $VO(O_iPr)_3$ anchoring to silica in the presence of isopropanol. Based on our isopropanol grafting studies with TMS-$SiO_{2(700)}$, we know that isopropanol reacts with strained siloxane bridges to form a silanol that donates a hydrogen bond to an adjacent ≡Si-O-$_i$Pr group. Based on ICP-OES and NMR data we know that $VO(O_iPr)_3$ can still react with these silanol groups to form monopodal sites that may exhibit weak coordination to the nearby ≡Si-O-$_i$Pr. Since isolated silanol groups and isopropanol are both hydrogen bond donors and acceptors, we envision two types of hydrogen bonding interactions between silanols and isopropanol in which isolated SiOH groups act as either an H-bond acceptor or donor for isopropanol (Scheme 3). We expect that H-bond donating silanols are still reactive anchoring sites (based on observations from our TMS-$SiO_{2(700)}$ grafting experiments), and that they react to form similar sites to those $VO(O_iPr)_3$ molecules that react with opened siloxane bridges. Given the single characteristic ^{51}V NMR peak for V+$_i$PrOH/$SiO_{2(700)}$, these vanadium sites must be nearby a ≡Si-O-$_i$Pr group.

We postulate that the decrease in vanadium loading for V+$_i$PrOH/$SiO_{2(700)}$ compared to V/$SiO_{2(700)}$ (Table 1, 2.1 wt.% V compared to 2.9 wt.% V, respectively) could be due to the decreased reactivity of hydrogen bond accepting silanols towards the $VO(O_iPr)_3$ precursor. Based on our isopropanol grafting studies we observe that upon post treatment of $SiO_{2(700)}$+$_i$PrOH, the IR spectrum for $SiO_{2(700)}$+$_i$POH$_{(50)}$ has decreased isolated silanol intensity relative to the original support, which could suggest the presence of some residual, strongly hydrogen bonded isopropanol to the silica surface. If some of these strongly hydrogen bound species are generated from silanols accepting H-bonds from isopropanol, then they could block $VO(O_iPr)_3$ molecules from reacting with the support when they are introduced in the second grafting step. In fact, we observe that residual H-bonded OH species remain in the IR spectrum for V+$_i$PrOH/$SiO_{2(700)}$ after $VO(O_iPr)_3$ grafting, while no such species are observed in the neat $VO(O_iPr)_3$ grafted material V/$SiO_{2(700)}$ (Figure S3). In contrast, all the H-bonded OH species are consumed in V+$_i$PrOH/TMS-$SiO_{2(700)}$, a material in which we expect all the silanols to be H-bond donating.

Comparison of $_i$PrOH and $VO(O_iPr)_3$ grafted to $SiO_{2(200)}$ and $SiO_{2(700)}$ supports.

While typical silica support pretreatment conditions for grafting chemistry involve dehydration at high temperatures to achieve dehydroxylation (> 350 °C),[9] silica is typically pretreated at temperatures far lower than 500 °C, if at all, for wet impregnation syntheses.[3] Therefore, during typical grafting experiments the surface of silica is comprised of sparse, isolated silanol groups, whereas during a typical wet impregnation the silica surface likely contains networks of hydrogen-bonded silanol nests. To this end, we grafted isopropanol and $VO(O_iPr)_3$ to $SiO_{2(200)}$ to determine the combined effect of coordinating solvent and hydrogen bonded silanols on the formation of silica-supported vanadium sites. We previously mentioned that isopropanol appears to have the opposite effect on $VO(O_iPr)_3$ anchoring to $SiO_{2(200)}$ compared to $SiO_{2(700)}$ (Table 1). Whereas vanadium content decreases on $SiO_{2(700)}$ when grafted in the presence of isopropanol, the vanadium content increases from

10.1002/chem.201904260

1.6 wt. % to 2.7 wt.% V when $VO(O_iPr)_3$ is grafted to $SiO_{2(200)}$ in the presence of isopropanol (Table 1). In this section, we characterize $V+_iPrOH/SiO_{2(200)}$ materials at length and compare them to their $V+_iPrOH/SiO_{2(700)}$ counterparts to elucidate the reason for their drastic differences in anchoring behavior.

Previously, we examined $VO(O_iPr)_3$ grafted to $SiO_{2(200)}$ with IR spectroscopy and found that all the isolated silanols reacted with $VO(O_iPr)_3$, whereas only a fraction of H-bonded silanols reacted and the remaining silanols were observed in the IR spectrum for $V/SiO_{2(200)}$.[5] We observed similar behavior in the IR spectrum for $V+_iPrOH/SiO_{2(200)}$ (Figure S3). Our prior work only addressed the detailed structural characterization of $VO(O_iPr)_3$ grafted to $SiO_{2(700)}$, however, solid-state NMR structural characterization of $VO(O_iPr)_3$ grafted to $SiO_{2(200)}$ without isopropanol present ($V/SiO_{2(200)}$) results in features in the ^{51}V NMR spectrum similar to those previously observed for $V/SiO_{2(700)}$, which are illustrated below the spectrum in Figure 4a. We will therefore limit our discussion to $VO(O_iPr)_3$ grafted to $SiO_{2(200)}$ with isopropanol present ($V+_iPrOH/SiO_{2(200)}$). The ^{51}V MAS NMR spectrum of $V+_iPrOH/SiO_{2(200)}$ in Figure 4a shows a single broad isotropic shift at –665 ppm, similar to the peak positions reported for the $V+_iPrOH/SiO_{2(700)}$ and $V+_iPrOH/TMS\text{-}SiO_{2(700)}$ materials. Simulation of the $V+_iPrOH/SiO_{2(200)}$ ^{51}V MAS NMR spectrum gives an isotropic linewidth of 5.2 kHz and a C_Q of 780 kHz (Figure S4, Table S1). Based on the isotropic chemical shift and C_Q we expect the vanadium sites on $V+_iPrOH/SiO_{2(200)}$ to have a similar structure to those suggested for $V+_iPrOH/SiO_{2(700)}$ and $V+_iPrOH/TMS\text{-}SiO_{2(700)}$ in Figure 3.

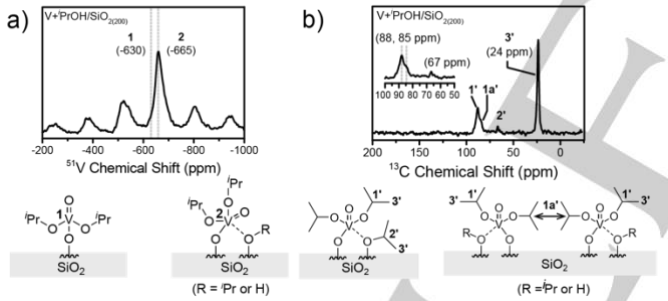

Figure 4. a) ^{51}V MAS NMR spectrum for isopropanol and $VO(O_iPr)_3$ grafted to $SiO_{2(200)}$ ($V+iPrOH/SiO_{2(200)}$) b) ^{13}C CP MAS NMR spectrum for $V+_iPrOH/SiO_{2(200)}$. Peak assignments are given below each spectrum.

Figure 4b shows the ^{13}C CPMAS NMR spectrum for $V+_iPrOH/SiO_{2(200)}$. The ^{13}C NMR spectrum for $V+_iPrOH/SiO_{2(200)}$ has one peak at 24 ppm labeled 3' and what appears to be two partially overlapped peaks at 85 ppm and 88 ppm labeled 1a' and 1', respectively. We assign signals 3' and 1'-1a' to the methyl carbons and the alpha carbon (most proximate to the oxygen) on a V-O-iPr moiety, respectively. A small additional peak at 67 ppm labeled 2' corresponding to the alpha carbon of the ≡Si-O-$_i$Pr group is also observed. We expect that isopropanol present during the synthesis of $V+_iPrOH/SiO_{2(200)}$ is the source of the small amount of ≡Si-O-$_i$Pr groups. The slight differences in chemical shift for the V-O-$_i$Pr alpha carbons 1a' and 1' are attributed to the spatial proximity of some V-O-iPr groups to other V-O-iPr moieties on neighboring vanadium sites (see structures in Figure 4b). Verification of these assignments are discussed in further detail with 2D NMR studies below.

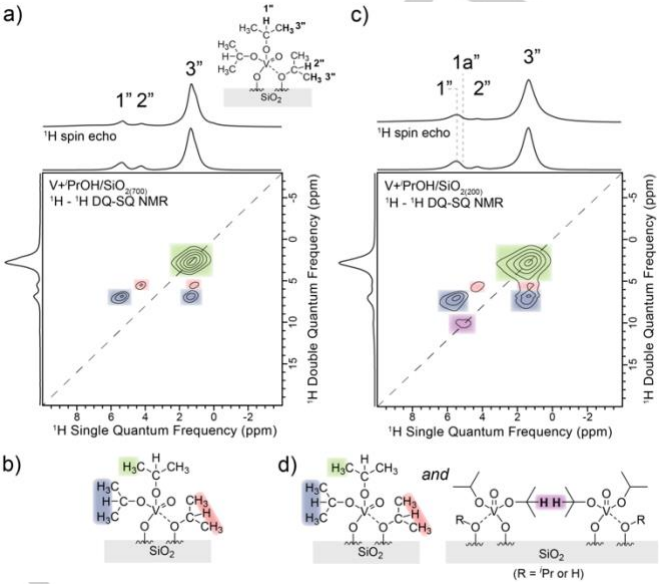

Figure 5. ^1H-^1H DQ-SQ 2D MAS NMR spectra for (a) $V+_iPrOH/SiO_{2(700)}$ and (b) structural assignments for observed cross peaks associated with the panel a spectrum, (c) $V+_iPrOH/SiO_{2(200)}$, and (d) structural assignments for observed cross peaks associated with the panel c spectrum.

Figure 5 compares ^1H-^1H Double Quantum-Single Quantum (DQ-SQ) 2D MAS NMR[12] spectra of $V+_iPrOH$ materials grafted to $SiO_{2(700)}$ and $SiO_{2(200)}$. For both spectra, the SQ frequency is provided on the horizontal axis and the DQ indirect dimension frequency is provided on the vertical axis. Auto-correlations arising from correlations between pairs of ^1H nuclei with the same chemical shift fall along the dashed line for which the SQ frequency is exactly half the DQ frequency. In Figure 5 panels a and c, the cross peak for signal 3" at 1.3 ppm in the SQ dimension and 2.6 ppm in the DQ dimension is attributed to an intramolecular DQ coherence between the methyl protons of the isopropoxide ligands (cross peaks are highlighted in green). The peak at 5.5 ppm in the DQ dimension is associated with an intramolecular DQ coherence between proton signals from ≡Si-O-$_i$Pr moieties labeled 2" and 3" in the SQ dimension (red cross peaks). The peak at 6.9 ppm in the DQ dimension corresponds to an intramolecular DQ coherence between protons from V-O-$_i$Pr moieties labeled 1" and 3" in the SQ dimension (blue cross peaks). These intramolecular coherence assignments are summarized in Figure 5b. While $V+_iPrOH/SiO_{2(700)}$ and $V+_iPrOH/SiO_{2(200)}$ share all of the aforementioned signals, $V+_iPrOH/SiO_{2(200)}$ contains an additional cross peak on the diagonal dotted line at 5 ppm in the SQ dimension and 10 ppm in the DQ dimension (signal 1a", Figure 5d, purple cross peak). This correlation is assigned to an intermolecular DQ coherence between V-O-iPr groups on two proximate vanadium sites. The close spatial proximity of some vanadium sites on the $SiO_{2(200)}$ support is expected given the

10.1002/chem.201904260

higher density of silanol groups and higher V loading on $SiO_{2(200)}$ compared to $SiO_{2(700)}$.

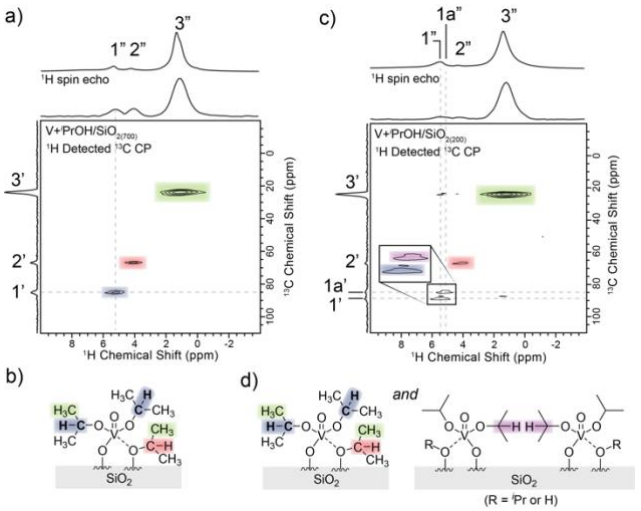

Figure 6. a) ^{1}H detected ^{13}C CP MAS NMR for V+$_i$PrOH/$SiO_{2(700)}$ and b) structural assignments for observed ^{1}H-^{13}C cross peaks, c) ^{1}H {^{13}C} CP-HETCOR NMR for V+$_i$PrOH/$SiO_{2(200)}$ and d) structural assignments or observed ^{1}H-^{13}C cross peaks. For both spectra, a projection of the 1D ^{1}H NMR spectrum with proton assignments is given on the horizontal axis, whereas the 1D ^{13}C NMR projection is given with assignments on the vertical axis.

The results from the 2D ^{1}H DQ-SQ NMR spectra of V+$_i$PrOH/$SiO_{2(200)}$ are crucial in that they enable us to resolve the resonance corresponding to spatially proximate V-O-$_i$Pr groups on adjacent vanadium sites. This helps inform further NMR analyses of differences in surface sites between V+$_i$PrOH/$SiO_{2(700)}$ and V+$_i$PrOH/$SiO_{2(200)}$. Figure 6 shows proton detected ^{1}H{^{13}C} 2D CP-HETCOR NMR spectra[13] for V+$_i$PrOH/$SiO_{2(700)}$ (panel a) and V+$_i$PrOH/$SiO_{2(200)}$ (panel c). The 1D projection ^{1}H spectrum is given on the horizontal axes; the 1D projection of the ^{13}C spectrum is given on the vertical axes. In the 2D ^{1}H-^{13}C spectrum for V+$_i$PrOH/$SiO_{2(700)}$, there are cross peaks between the ^{1}H signal labeled 1" and the ^{13}C signal labeled 1', ^{1}H signal 2" and ^{13}C signal 2', and ^{1}H signal 3" and ^{13}C signal 3'. Visual representation of these cross-peak assignments is given in Figure 6b. As expected, each of these cross peaks corresponds to the correlation between ^{13}C nuclei from a V-O-$_i$Pr group (1' and 3') or S-O-$_i$Pr group (2' and 3') and the ^{1}H nuclei directly bound to those carbons.

Figure 6c shows the ^{1}H{^{13}C} 2D CP-HETCOR NMR spectrum of V+$_i$PrOH/$SiO_{2(200)}$. This spectrum shares the same three main cross peaks as those observed in the ^{1}H-^{13}C spectrum for V+$_i$PrOH/$SiO_{2(700)}$, however there is an additional cross peak between a ^{1}H signal at ~5 ppm (1a") and ^{13}C signal at 83 ppm (1a'). We assign the 1a" – 1a' cross peak to a correlation between ^{1}H and ^{13}C nuclei on a V-O-$_i$Pr groups that are spatially proximate to other vanadium sites (see illustration in Figure 6d). This assignment is also based upon the correlation observed in the 2D ^{1}H-^{1}H DQ-SQ spectrum (see above and Figure 5c). From this we again conclude that there are two slightly different vanadium sites on V+$_i$PrOH/$SiO_{2(200)}$: (i) those vanadium nuclei which are primarily isolated (like the sites from V+$_i$PrOH/$SiO_{2(700)}$, and (ii) those which are sufficiently proximate to other vanadium sites such that an interaction between neighboring V-O-$_i$Pr groups can be observed. This observation that the ^{51}V isotropic peak for V+$_i$PrOH/$SiO_{2(200)}$ exhibits nearly double the linewidth compared to V+$_i$PrOH/$SiO_{2(700)}$ (5.2 kHz compared to 2.8 kHz, Table S1) could be explained by the greater variation in the heterogeneity of surface vanadium sites for V+$_i$PrOH/$SiO_{2(200)}$.

Although we suspect that silanols accepting hydrogen bonds from isopropanol on $SiO_{2(700)}$ can have a detrimental effect on the ability of $VO(O_iPr)_3$ to anchor to silica, we expect that hydrogen bonding between isopropanol and hydrogen bonded silanol nests on $SiO_{2(200)}$ must create some favorable interaction that enables the increased $VO(O_iPr)_3$ anchoring to the support surface. Scheme 4 illustrates a proposed pathway in which isopropanol could interact with hydrogen bonded silanol nests to increase the number of anchoring sites. This illustration is, of course, an oversimplification of the support surface to demonstrate our point more clearly and to highlight the practical implications of this study for catalyst preparation. The top panel of this illustration shows a chain of hydrogen bonded silanols that represents a hydrogen bonded silanol nest. The silanol at the edge of the silanol nest is only hydrogen bond donating, and therefore is still a viable anchoring site (hence the green check mark below that site). The rest of the silanols in the interior of this chain are accepting hydrogen bonds from other silanols and therefore have reduced reactivity towards the $VO(O_iPr)_3$ precursor. This could explain why some, but not all, of the H-bonded silanols are reactive towards $VO(O_iPr)_3$ on $SiO_{2(200)}$. When an isopropanol molecule comes within hydrogen bonding distance with this silanol nest, however, it is possible that it can

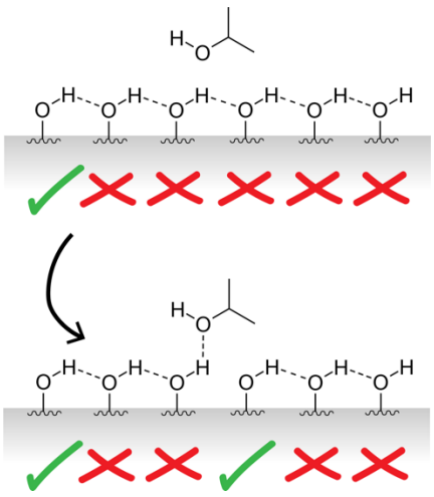

Scheme 4. Illustration of hypothesized disruption of silanol nests and subsequent formation of anchoring sites on silica via hydrogen bonding between silanols and isopropanol: Practical implications for catalyst preparation.

accept a hydrogen bond from one of the silanol groups on the interior of the silanol nest. This would in turn disrupt the hydrogen

10.1002/chem.201904260

bonding network within the silanol nest and create a new silanol group that is accessible for anchoring by the $VO(O_iPr)_3$ precursor. In the ^{13}C CPMAS spectrum for V+$_i$PrOH/$SiO_{2(200)}$ we do observe an increase in Si-O-$_i$Pr species and an increase in the number of V-O-$_i$Pr moieties that appear to be proximate to other nearby isopropoxide groups (and not just H-bonded silanols), which could be evidence for this mechanism taking place on V+$_i$PrOH/$SiO_{2(200)}$.

Although isopropanol -OH can potentially create favorable hydrogen bond interactions in which they accept a hydrogen bond from surface silanol nests, we have seen they can also create unfavorable interactions in which they donate a hydrogen bond to surface silanols and therefore detract from the reactivity of those silanols. Therefore, a different small molecule that could act solely as a hydrogen bond acceptor could potentially serve as a better solvent to increase vanadium anchoring to the silica surface. To this end, we performed a two-step grafting experiment in which we replaced isopropanol in the first grafting step with 2-butanone. 2-butanone contains a ketone group which can act only as a hydrogen bond acceptor, and it has a similar boiling point to isopropanol. Because this molecule cannot create the hydrogen bond donating interactions that detract from $VO(O_iPr)_3$ anchoring, we expect that it will further increase the amount of $VO(O_iPr)_3$ to the $SiO_{2(200)}$ surface. Indeed, the two-step grafted 2-butanone material (V+2-butanone/$SiO_{2(200)}$) contains 4.4 ± 0.2 wt.% vanadium, which is a significant increase from the 2.6 wt. % V on V+$_i$PrOH/$SiO_{2(200)}$. Following the detailed study of these grafted materials, we verified that all the materials in this study form dispersed, two-dimensional VO_x sites following calcination at 550 °C in air with Raman spectroscopy and solid-state ^{51}V MAS NMR for select samples (Figures S7 and S8).

Conclusions

In this study, we used vapor phase deposition techniques to synthesize and systematically investigate the influence of solvent on the dispersion of vanadium oxide on silica. To this end, we grafted isopropanol and $VO(O_iPr)_3$ in subsequent steps to silica supports dehydrated at 200 °C and 700 °C ($SiO_{2(200)}$ and $SiO_{2(700)}$). We compared the extent of $VO(O_iPr)_3$ anchoring to these supports in the presence of isopropanol with ICP-OES and found that compared to grafting without isopropanol, vanadium content decreases when $VO(O_iPr)_3$ is grafted to $SiO_{2(700)}$ in the presence of isopropanol, yet vanadium content increases when $VO(O_iPr)_3$ is grafted to $SiO_{2(200)}$ in the presence of isopropanol. We also grafted isopropanol and $VO(O_iPr)_3$ to silylated silica (TMS-$SiO_{2(700)}$) in which all of the isolated silanol groups were blocked. We found that isopropanol reacts with strained siloxane bridges on the surface of this material to form a ≡Si-O-$_i$Pr group adjacent to a SiOH group. Although FTIR spectroscopy confirms that this SiOH group is hydrogen bonded to the adjacent ≡Si-O-$_i$Pr, the $VO(O_iPr)_3$ group can still react with this SiOH. In fact, the vanadium content on V+$_i$PrOH/TMS-$SiO_{2(700)}$ is the same as the material where only $VO(O_iPr)_3$ is grafted to TMS-$SiO_{2(700)}$ (V/TMS-$SiO_{2(700)}$).

These results lead us to a model where we describe the reactivity of the SiO_2 surface towards $VO(O_iPr)_3$ in terms of the hydrogen bonding character of the surface SiOH groups. If a silanol group on silica is donating a hydrogen bond to either another silanol group, a ≡Si-O-$_i$Pr group, or to an isopropanol molecule, it is still a sufficiently reactive anchoring site for the $VO(O_iPr)_3$ precursor. However, if a silanol group is accepting a hydrogen bond either from a solvent molecule or another silanol group it will not be a viable anchoring site for $VO(O_iPr)_3$.

This model for the description of dispersion of $VO(O_iPr)_3$ could be used to inform the synthesis of supported vanadium oxide (and potentially other metal oxides synthesized with an analogous procedure) materials with improved dispersion. The incorporation of solvent molecules with exclusively hydrogen bond accepting capabilities into the wet impregnation synthesis of supported metal oxides could potentially help to disrupt the hydrogen bonding interactions in silanol nests on the silica support and make these silanol groups more reactive towards the metal oxide precursor molecules. As a preliminary demonstration, we observed that the presence of 2-butanone during $VO(O_iPr)_3$ grafting can increase the extent of precursor anchoring to the $SiO_{2(200)}$ silica surface. We believe that this type of hydrogen bonding disruption could also help to explain why doping the surface of silica with Na^+ ions reported previously by our group can lead to significant improvements in group V metal oxide dispersion.[1, 14]

Experimental Section

Material synthesis

Grafting: $SiO_{2(700)}$, $SiO_{2(200)}$, and TMS-$SiO_{2(700)}$ supports were prepared by the procedure described elsewhere.[5] Anhydrous isopropanol (Sigma-Aldrich) was deposited onto 300 mg of thermally pretreated silica (20 equiv based on initial silanol content) at ca. 20 µbar dynamic vacuum. The transfer phase was followed by a reaction phase at room temperature (30 min) and a mild thermal post-treatment at 50 °C and 20 µbar dynamic vacuum for 1h in order to evaporate excess isopropanol (materials denoted as $SiO_{2(X)+iPrOH}$).

Anhydrous isopropanol (Sigma-Aldrich) was deposited onto 300 mg of thermally pretreated silica (20 equiv based on initial silanol content) at ca. 20 µbar dynamic vacuum. The transfer phase was followed by a reaction phase at room temperature (30 min). Following this step the pretreated silica reactor was sealed and the isopropanol precursor container was switched for a $VO(O_iPr)_3$ precursor container. $VO(O_iPr)_3$ (Sigma-Aldrich, distilled two times before use, colorless) was deposited onto the isopropanol + pretreated silica mixture (5 equiv based on initial silanol content) at ca. 20 µbar dynamic vacuum. The transfer phase (1 h) was followed by a reaction phase at room temperature (30 min) and a mild thermal post-treatment at 50 °C and 20 µbar dynamic vacuum for 1h in order to evaporate excess isopropanol and $VO(O_iPr)_3$.

Characterization

Infrared spectra were recorded on a self-supporting wafer using a Bruker Alpha spectrometer in transmission mode (resolution of 2 cm^{-1}). Intensities were normalized to the Si–O–Si overtones of the silica framework. Analysis was carried out inside a glovebox (<1 ppm of H_2O and O_2).

Thermogravimetric analysis-differential scanning calorimetry-mass spectrometry of the calcination step was performed using a TGA-DSC

10.1002/chem.201904260

Thermobalance (LINSEIS) in combination with an OmniStarTM mass spectrometer (Pfeiffer Vacuum). 15-20 mg of SiO_2+iPrOH sample was sealed in an aluminum sample pan inside a glovebox (<1 ppm of O_2 and H_2O) prior to TGA-DSC-MS analysis. Samples were heated to 550 C (20 °C min_{-1} ramp) in air (or N_2) with a flow rate of 20 mL min_{-1} inside the TGA-DSC furnace during sample analysis.

Inductively Coupled Plasma-Optical Emission Spectroscopy. 15-20 mg of vanadium-functionalized material was digested with 200 uL of 48 wt.% HF. The digested samples were diluted with 20 mL 4 wt. % boric acid solution (Honeywell) and 10 mL Milli Q water. The vanadium content was quantified with the ICP-OES (Optima 2000 DV from PerkinElmer) instrument.

Solid-State NMR. Solid-state NMR experiments on V+*i*PrOH/$SiO_{2(700)}$, V+*i*PrOH/TMS-$SiO_{2(700)}$, and V+*i*PrOH/$SiO_{2(200)}$ were performed on a Bruker widebore 9.4 T NMR magnet equipped with a Bruker 2.5 mm triple resonance probe and a Bruker Avance III HD console. Recycle delays between 0.18 and 2 seconds were used for all experiments. ^{1}H radio frequency (rf) pulse calibrations were directly performed on each sample. Direct excitation ^{51}V NMR spectra of V+*i*PrOH/$SiO_{2(700)}$, V+*i*PrOH/TMS-$SiO_{2(700)}$, V+*i*PrOH/$SiO_{2(200)}$ were acquired with a 15 kHz MAS frequency and a 0.781 µs CT-selective excitation pulse was used. MAS frequencies of 15 kHz and 25 kHz were used to verify spinning sidebands. Only the data from 15kHz MAS is shown. Direct excitation ^{51}V NMR Spectra were acquired at two MAS frequencies to confirm the position of the isotropic peaks. The ^{51}V CT-selective pulse widths were calculated from ^{13}C pulse widths. The number of scans used were 16,384, 66,428, 53,248, and 139,264 for V+*i*PrOH/$SiO_{2(700)}$, V+*i*PrOH/TMS-$SiO_{2(700)}$, V+*i*PrOH/$SiO_{2(200)}$, and V+*i*PrOH/$SiO_{2(200)}$-O2, respectively. Proton-detected CP-HETCOR[13] experiments used 2.5 ms/2.5 ms and 12 ms/6 ms front/back contact times for ^{13}C and ^{29}Si, respectively, with the forward and backward CP steps using a rf ramp from 85-100% on the ^{1}H spin-lock pulse. CP contact powers were directly optimized on each sample. ^{1}H decoupling using the SPINAL-64 scheme[15] was applied at 100 kHz for CP experiments. Proton detected ^{51}V→^{1}H 2D HETCOR NMR spectra were obtained with the D-RINEPT pulse sequence.[16] $SR4_1^2$ heteronuclear ^{1}H recoupling[17] was applied with an rf field of twice the MAS frequency (50 kHz). Each $SR4_1^2$ block was 480 µs in duration. ^{1}H DQ-SQ 2D dipolar homonuclear correlation NMR spectra were obtained with the BABA pulse sequence.[18] Each BABA recoupling block was one rotor cycle (40 µs) in duration. CP, D-RINEPT and DQ NMR experiments were performed with a MAS frequency of 25 kHz. See Table S2 for the acquisition parameters of the 2D experiments.

Raman Spectroscopy. All Raman measurements were performed with a Renishaw InVia Raman Spectrometer using a 785 nm excitation laser equipped with a 1200 l mm_{-1} grating, and a dispersion of 1.36565 cm_{-1} $pixel_{-1}$. All measurements were performed at ambient conditions.

Acknowledgements

Materials synthesis and characterization other than solid-state NMR (A.M.L., M.C.C., P.U., and I.H.) were supported by the National Science Foundation under Grant No. CBET-1605101. Solid-state NMR spectroscopy experiments (S.L.C, M.P.H and A.J.R.) were supported by the U.S. Department of Energy (DOE), Office of Science, Basic Energy Sciences, Materials Science and Engineering Division. The Ames Laboratory is operated for the U.S. DOE by Iowa State University under Contract No. DE-AC02-07CH11358.

Keywords: supported catalysts • heterogeneous catalysis • solid state NMR • vanadium • oxidative dehydrogenation

[1] J. T. Grant, C. A. Carrero, A. M. Love, R. Verel, I. Hermans, *ACS Catalysis* **2015**, *5*, 5787-5793.

[2] a) C. A. Carrero, C. J. Keturakis, A. Orrego, R. Schomacker, I. E. Wachs, *Dalton Transactions* **2013**, *42*, 12644-12653; b) J. T. Grant, A. M. Love, C. A. Carrero, F. Huang, J. Panger, R. Verel, I. Hermans, *Topics in Catalysis* **2016**, *59*, 1545-1553.

[3] E. Marceau, X. Carrier, M. Che, O. Clause, C. Marcilly, in *Handbook of Heterogeneous Catalysis* (Ed.: Wiley), **2008**.

[4] a) S. Barman, N. Maity, K. Bhatte, S. Ould-Chikh, O. Dachwald, C. Haesner, Y. Saih, E. Abou-Hamad, I. Llorens, J.-L. Hazemann, K. Kohler, V. D'Elia, J.-M. Basset, *ACS Catal.* **2016**, *6*, 5908-5921; b) M. P. Hogerl, L. M. S. Goh, E. Abou-Hamad, S. Barman, O. Dachwald, F. A. Pasha, J. Pelletier, K. Kohler, V. D'Elia, L. Cavallo, J.-M. Basset, *RSC Adv.* **2018**, *8*, 20801-20808; c) H. Zhu, S. Ould-Chikh, H. Dong, I. Llorens, Y. Saih, D. H. Anjum, J.-L. Hazemann, J.-M. Basset, *ChemCatChem* **2015**, *7*, 3332-3339; d) A. Gervasini, P. Carniti, J. Keränen, L. Niinistö, A. Auroux, *Catal. Today* **2004**, *96*, 187-194; e) J. Keränen, A. Auroux, S. Ek, L. Niinistö, *Appl. Catal., A* **2002**, *228*, 213-225; f) J. Keranen, C. Guimon, E. Iiskola, A. Auroux, L. Niinisto, *J. Phys. Chem. B* **2003**, *107*, 10773-10784; g) J. Keranen, P. Carniti, A. Gervasini, I. Eero, A. Auroux, L. Niinisto, *Catalysis Today* **2004**, *91-92*, 67-71; h) J. A. N. Ajjou, G. L. Rice, S. L. Scott, *Journal of the American Chemical Society* **1998**, *120*, 13436-13443; i) G. L. Rice, S. L. Scott, *Langmuir* **1997**, *13*, 1545-1551; j) K. Inumaru, T. Okuhara, M. Misono, *J. Phys. Chem.* **1991**, *95*, 4826-4832; k) S. L. Wegener, H. Kim, T. J. Marks, P. C. Stair, *The Journal of Physical Chemistry Letters* **2011**, *2*, 170-175; l) P. Mania, S. Conrad, R. Verel, C. Hammond, I. Hermans, *Dalton Transactions* **2013**, *42*, 12725-12732.

[5] A. M. Love, C. A. Carrero, A. Chieregato, J. T. Grant, S. Conrad, R. Verel, I. Hermans, *Chemistry of Materials* **2016**, *28*, 5495-5504.

[6] M. Deni, C.-V. Aleix, C. Christophe, *ChemRxiv* **2019,** Preprint.

[7] a) L. T. Zhuravlev, *Colloids and Surfaces A: Physicochemical and Engineering Aspects* **2000**, *173*, 1-38; b) C. S. Ewing, S. Bhavsar, G. Veser, J. J. McCarthy, J. K. Johnson, *Langmuir* **2014**, *30*, 5133-5141.

[8] a) P. Hoffmann, E. Knözinger, *Surface Science* **1987**, *188*, 181-198; b) A. Rimola, D. Costa, M. Sodupe, J.-F. Lambert, P. Ugliengo, *Chemical Reviews* **2013**, *113*, 4216-4313.

[9] M. A. Natal-Santiago, J. A. Dumesic, *J. Catal.* **1998**, *175*, 252-268.

[10] P. J. Linstrom, W. G. Mallard, National Institute of Standards and Technology, Gaithersburg, MD.

[11] O. B. Lapina, V. M. Mastikhin, A. A. Shubin, V. N. Krasilnikov, K. I. Zamaraev, *Progress in Nuclear Magnetic Resonance Spectroscopy* **1992**, *24*, 457-525.

[12] a) H. Geen, J. J. Titman, J. Gottwald, H. W. Spiess, *Chem. Phys. Lett.* **1994**, *227*, 79-86; b) F. Blanc, C. Copéret, A. Lesage, L. Emsley, *Chemical Society Reviews* **2008**, *37*, 518-526.

[13] J. W. Wiench, C. E. Bronnimann, V. S. Y. Lin, M. Pruski, *J. Am. Chem. Soc.* **2007**, *129*, 12076-12077.

[14] R. J. Chimentao, J. E. Herrera, J. H. Kwak, F. Medina, Y. Wang, C. H. F. Peden, *Appl. Catal., A* **2007**, *332*, 263-272.

[15] B. M. Fung, A. K. Khitrin, K. Ermolaev, *Journal of Magnetic Resonance* **2000**, *142*, 97-101.

[16] a) A. Venkatesh, M. P. Hanrahan, A. J. Rossini, *Solid State Nuclear Magnetic Resonance* **2017**, *84*, 171-181; b) J. Trebosc, B. Hu, J. P. Amoureux, Z. Gan, *Journal of Magnetic Resonance* **2007**, *186*, 220-227.

[17] A. Brinkmann, A. P. M. Kentgens, *J. Am. Chem. Soc.* **2006**, *128*, 14758-14759.

[18] M. Feike, D. E. Demco, R. Graf, J. Gottwald, S. Hafner, H. W. Spiess, *Journal of Magnetic Resonance, Series A* **1996**, *122*, 214-221.

10.1002/chem.201904260

WILEY-VCH

Entry for the Table of Contents (Please choose one layout)

Layout 1:

FULL PAPER

Disrupting the H-bonding network generates more reactive anchoring sites on silica.

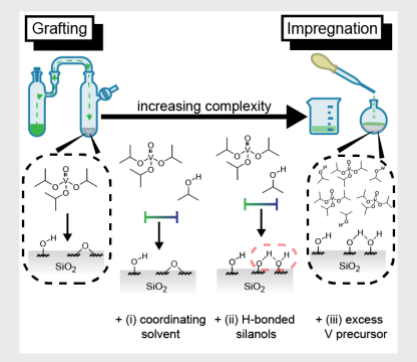

Alyssa M. Love,[‡][a] Melissa C. Cendejas,[‡][a] Michael P. Hanrahan,[c] Scott L. Carnahan,[c] Pajean Uchupalanun,[a] Aaron J. Rossini,[c] Ive Hermans[a],[b],**

Page No. – Page No.

Understanding the Synthesis of Supported Vanadium Oxide Catalysts using Chemical Grafting